NANODAY@PENN 2007

GRADUATE Research

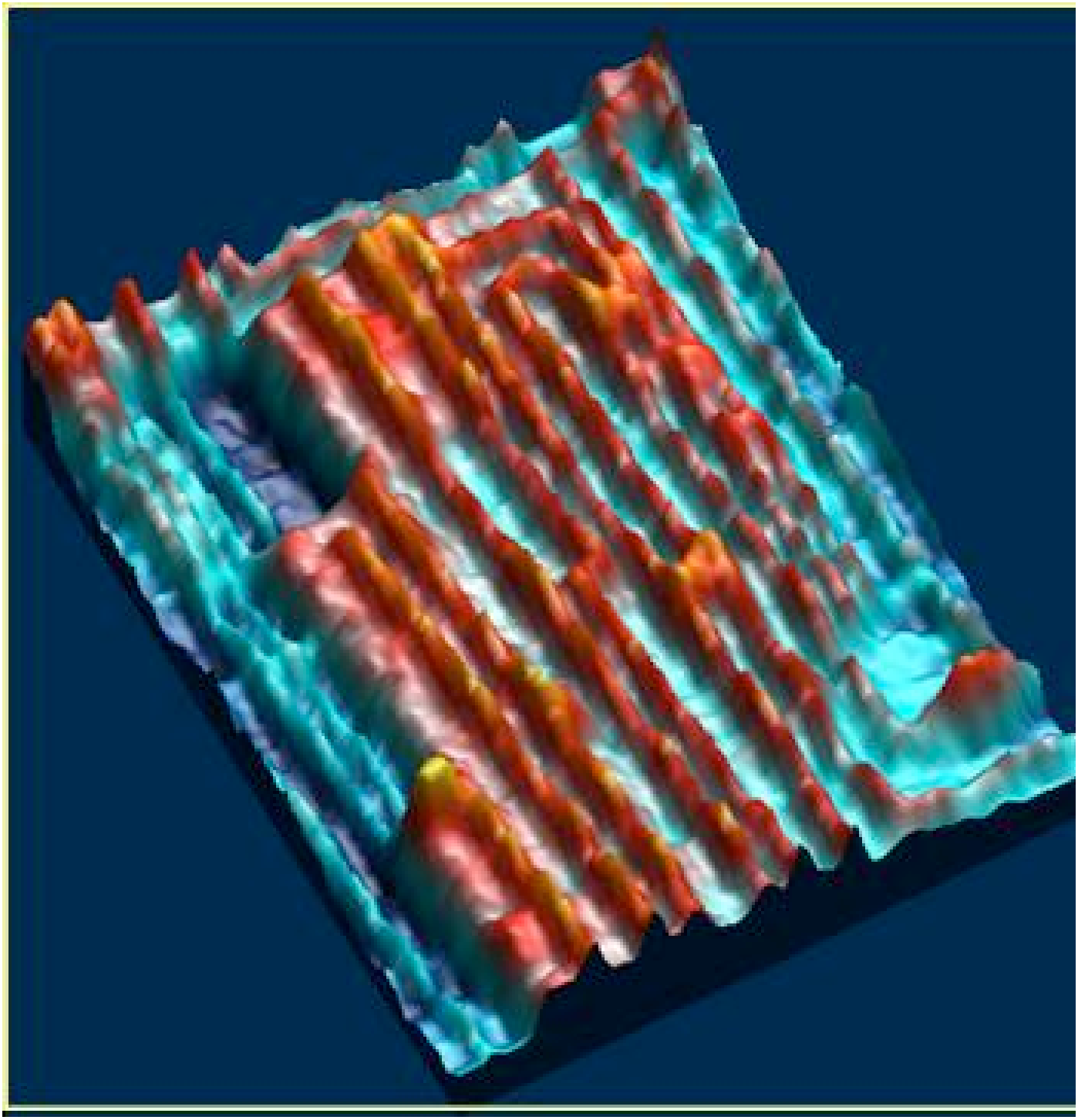

Nanostripes developed on $BaTiO_3$ surface by NC-AFM, Dongbo Li and Dawn Bonnell

NANO / BIO INTERFACE CENTER

NBIC Graduate Student Poster Session at NanoDay@ Penn 2007

RAISLER LOUNGE, TOWNE BUILDING
2:00 - 4:00 PM

1. The mechanics and behavior of actin filaments in an electric field
Mark E. Arsenault, Hui Zhao, Prashant K. Purohit, Yale E. Goldman, Haim H. Bau

With the aid of AC electric fields ("electric tweezers"), we suspended rhodamine-phalloidin labeled actin filaments between two electrodes separated by a 5 mm gap and elevated 1.3 mm above a glass surface. This technique provided a convenient, stable geometry for observing the thermal fluctuations of the filaments. The root-mean-squared lateral displacement (Drms) of the filament was measured as a function of the distance from the anchoring electrodes. At 37 mM KCl, and with applied electrical frequency of 2 MHz, the midpoint Drms was 151 ± 14 nm (s.e.m.) at 4 V peak-to-peak voltages and decreased to 43.2 ± 6.0 nm at 12 V. This strong effect of V on the thermal fluctuations indicates a change in the flexural rigidity and/or an axial tension imposed, directly or indirectly, by the electric field. Tension might be produced by an electric body force (electrostriction), induced electrohydrodynamics (electro-osmosis), or joule heating. A simple linear Brownian dynamic model was derived to express Drms as a function of flexural rigidity, tension, and location along the filament. On the preliminary assumption that only the tension depends on the electric field intensity, and using an established value for the persistence length (17 mm), the apparent voltage-induced filament tension increased linearly with V2, as expected from the mechanisms listed above. The experimental method developed in this work provides a means to reliably measure filament thermal fluctuations under altered ambient conditions and to study the effect of filament tension on the processive motion of myosin motors.

2. Twirling of Actin by Myosin

John F. Beausang, John Lewis, Harry T. Schroeder III, H. Lee Sweeney, Yale E. Goldman

Several factors are expected to determine whether actin experiences a torque during active myosin-directed sliding: the direction of the force vector between actin and myosin, the distribution of myosin binding sites on actin, and cooperation between myosins translocating an individual actin filament. Consequently, studies in the literature have disagreed on whether myosin moves axially along actin or helically with a right-handed or left-handed pitch. Different results are obtained from muscle myosin and various unconventional myosin isoforms. We have developed a new assay to monitor azimuthal rotation of actin in a gliding filament assay using polarized total internal reflectance fluorescence microscopy. The actin is sparsely labeled with tetramethylrhodamine at Cys374 and the three-dimensional orientation of the individual rhodamines is monitored during in vitro filament gliding with 40-80 ms time resolution. To determine the handedness of any twisting motions, extra ± 45° excitation polarizations were added to our earlier single molecule fluorescence polarization method. During translocation by myosin, approximately half of the observed actin filaments exhibit a 'twirling' helical path of rotation around the filament axis. Native myosin II and V consistently induce a left-handed twirling motion (opposite to the long-pitch helix of actin) with pitch 1.0 ± 0.2 μm for myosin II and 1.7 ± 0.1 μm for myosin V. Full-length (6 IQ motifs) and truncated (4 IQ) recombinant myosin V predominately twirl with left-handed pitches of 1.4 ± 0.2 μm and 1.2 ± 0.2 μm, respectively. The 4 IQ myosin motifs exhibit an increased fraction of right-hand twirlers and fewer "non-twirling" molecules compared to the 6 IQ myosin. Myosin VI, however, twirls with a predominately right-handed pitch of 1.2 ± 0.1 μm. The observed twirling motions may be the result of an applied torque between the two proteins that is required in some theories of actomyosin motility.

3. Hybrid Fluorescence and Atomic Force Microscopy: Specificity, Resolution, and Force for Biophysics and Cell Biology

André E.X. Brown, Alina Popescu, Henry Shuman, Dennis E. Discher

Fluorescence and atomic force microscopy (AFM) have both independently become important tools in the study of cell and molecular biophysics. It is now possible to combine the strengths of these two methods in one hybrid instrument. The most obvious advantage of this approach is that it combines the high resolution of AFM with the chemical specificity and time resolution of fluorescence microscopy. In addition to higher resolution we show that information can be derived from a quantitative comparison of the complementary data that would be unavailable from either method alone or, as far as we know, from any other method. Finally, because AFM images are formed using a flexible cantilever whose deflection can be accurately measured, it is possible to make quantitative force measurements. When combined with fluorescence microscopy to visualize the resulting sample deformations, the hybrid instrument opens up new regimes for measuring highly extensible biological materials.

4. Integrating different types of nanowire sensors in a large array — An Approach to Electronic Noses
Yaping Dan, Stephane Evoy, A.T. Charlie Johnson

Biological noses have a key structural feature: different types of sensors in a large array. Human noses, for example, have around 100 types of sensing cells with 100,000 cells of each type. To mimic the functions of the biological noses, electronic noses must possess this feature. However, it is a big challenge to obtain this feature even with today's technology.

In this poster, we demonstrate a simple and low-cost approach to integrate different types of nanowire sensors in a large array on the same silicon wafer. We first fabricate an array of PMMA nano-ribbons with each contacting a prefabricated gold electrode using nano imprint technology. Spin-On-Glass (SOG) will then be spin-coated on the nano-ribbon array. After baking at ~500C for 1h, SOG will turn into silicon oxide and PMMA nano-ribbons into gaseous residues at the same time. Nano-channels are thus formed.

It has been demonstrated that electroplating is an excellent synthesis method to grow various kinds of nanowires such as metallic, ceramic, semi-conductive and conducting polymeric nanowires, a lot of which are also good candidates for sensing applications. Using this method, nanowires can be grown in the above-mentioned nanochannel array. Moreover, this design allows for addressable simultaneous synthesis of a specific type of nanowire in specified channels by providing the voltage to the electrodes connecting to those channels. This process can be further repeated to produce different types of nanowires in other channels using different electroplating solutions.

With this method, we can fabricate a large array consisting of many different types of nanowires. The scale of this array can compete with that of biological noses and their functions are expected to be comparable to those of biological noses too. This method involves lithography technology only one time for the prefabricated gold electrode array. It is cost-effective enough for commercialization.

5. Interfacial Assembly of Nanoparticles in Discrete Block-Copolymer Aggregates
Brenda Sanchez-Gaytan, Timothy Duncan, Weihong Cui, YooJin Kim, Miguel Mendez-Polanco, Michael Fryd, Bradford B. Wayland, So-Jung Park

The cooperative self-assembly of CdSe nanoparticles and amphiphilic block-copolymers led to a unique radial arrangement of nanoparticles at an interface inside discrete block-copolymer aggregates. It was found that the presence of nanoparticles induces a drastic morphology change of block-copolymer aggregates rather than being incorporated passively as simple solutes. The nanoparticles in block-copolymer aggregates were highly luminescent showing promise for biological imaging applications.

6. Interactions between diblock copolymer and ferritin within synthetic polymer vesicles
Masaya Jimbo, Ivan Dmochowski

Polymersomes – synthetic analogues of liposomes – are ideal platforms for targeted delivery and imaging due to their great mechanical strength, tunable membrane properties, and large aqueous cores. These vesicles show potential for delivery of therapeutic proteins that either denature easily or have short half-lives in the blood stream.

Ferritin, a ubiquitous family of hollow iron storage proteins, was chosen to demonstrate the ability of polymersomes to encapsulate proteins, due to its complex structure and remarkable stability over a wide range of pH and temperatures. It is made up of 24 subunits (4-helix bundles) and can store up to 4500 iron atoms in the ferric state. Ferritin and its iron-lacking variant apoferritin were labeled with either Cy3 or BODIPY iodoacetamide, encapsulated in porphyrin-labeled polymersomes, and imaged using confocal microscopy.

Our results demonstrate that encapsulated BODIPY-labeled (apo)ferritin localizes to the inner membrane surface, whereas Cy3-labeled (apo)ferritin is found both at the membrane and diffused throughout the aqueous core. Protein encapsulation causes vesicle morphology to change from predominantly spherical structures to a mixture of elongated and bead-like structures. Moreover, laser illumination results in vesicle shape changes and/or budding of smaller vesicles. (Apo)ferritin-loaded polymersomes possess altered mechanical properties, as application of mechanical stress via micropipette aspiration demonstrates an increased elastic modulus for an entire vesicle population.

7. Probing the Structure of DNA-Carbon Nanotube Hybrids with Molecular Dynamics
Robert R. Johnson, A.T. Charlie Johnson, Michael L. Klein

DNA-carbon nanotube hybrids (DNA-NT) are novel nanoscale materials that consist of single walled carbon nanotubes (SWNT) coated with a self-assembled monolayer of single stranded DNA (ssDNA). Many recent experiments involving DNA-NT have shown that this material is an excellent candidate for chemical and biological sensing applications. Despite the significance of DNA-NT, a detailed understanding of its microscopic structure and interactions is lacking. To address these issues we have performed classical all-atom molecular dynamics (MD) simulations. MD reveals the nature of the interactions and structural arrangements involved in DNA-NT. We find that the hybrid material spontaneously self-assembles in aqueous solution via the p-p stacking interaction between ssDNA nucleobases and SWNT outer wall. Under ambient conditions, ssDNA can adopt various wrapping conformations about SWNT including right- and left-handed helices and achiral loops. Simulations of a (GT)7 - Nanotube hybrids, reveal the nature of sequence dependent DNA conformations which has interesting connections to DNA-NT chemical sensors.

8. Parallel Fabrication and Real-Time TEM Imaging of the Formation of Crystalline Nano-scale Gaps
Danvers E. Johnston, Douglas R. Strachan Beth S. Guiton, Peter K. Davies, Dawn A. Bonnell, A. T. Charlie Johnson

We have developed a technique for simultaneously fabricating large numbers of nanogaps in a single processing step using feedback-controlled electromigration. Parallel nanogap formation is achieved by a balanced simultaneous process that uses a novel arrangement of nanoscale shorts between narrow constrictions where the nanogaps form. Due to this balancing, the fabrication of multiple nano-electrodes is similar to that of a single nanogap junction. Additionally, we present real-time transmission electron microscopy (TEM) of nanogap formation by feedback-controlled electromigration (FCE) that reveals a remarkable degree of crystalline order. The technique should be useful for constructing complex circuits of molecular-scale electronic devices.

9. Single Stranded DNA-Single-Walled Carbon Nanotube Sensors For Detection Of Gaseous Analytes
Samuel Khamis[1], Michelle Chen[2], Robert Johnson[1], A.T. Charlie Johnson[1]

Recently there has been great interest in sensing strategies based on tuning the chemical affinity of single walled carbon nanotube field effect transistors (SWNT FET's). We have demonstrated a versatile family of vapor sensors based on single stranded DNA as the chemical recognition site and SWNT FET's as the electronic readout component. This combination is particularly intriguing because of the chemical compatibility of these two nanostructures, and the chemical diversity of the ssDNA. We have demonstrated the utility of such devices for vapor sensing [1], and report here on results involving more than a dozen different ssDNA sequences. Our gas panel includes chemicals found in explosives, neurotoxins, and disease defining compounds. ssDNA/SWNT sensors are sensitive to these analytes at concentrations of parts per million, and our library of sensing responses along with the number of ssDNA sequences we have tested show a clear "footprint" for each of the analytes to our sensor. These devices lend themselves to use in an electronic nose (e-nose) system, where a large sensor array is coupled to signal-conditioning electronics and sensor responses fed to odor recognition algorithms to perform detection and classification of vapors.

We have established that ssDNA base sequence is the controlling parameter for sensor response by fabricating sensors using ssDNA oligomers with the same base content but different base ordering. Figure 1 shows the different responses of our sensors to Dimethyl methylphosphonate (DMMP) (a sarin simulant) with the same bases in different configurations. Given the very large number of different ssDNA sequences, this observation opens up possibility of creating the large number of sensors with widely varying response characteristics that are needed for an e-nose sensor array.

10. Interaction Between Single-Walled Carbon Nanotubes and Water Soluble, Rigid Rod-like Poly(p-phenyleneethynylene)

One-Sun Lee, Youn K. Kang, Tae-Hong Park, Sang Hoon Kim, Pravas Deria,
Dawn A Bonnell, Michael J. Therien, Jeffery G. Saven

The dispersal and solubization of carbon nanotubes is necessary for their processing and manipulation. Recently, new amphiphilic linear conjugated polymers, poly[p-{2,5-bis(3-propoxysulfonicacidsodiumsalt)}phenylene]ethynylene (PPES), have been synthesized that show improved solubility properties over standard surfactants. Single wall nanotubes (SWNT) were dispersed after 3 hours of sonication with the mass percent conversion of 70%, as revealed by visible and near-infrared absorption spectroscopy and by atomic force microscopy (AFM). Despite rigid, rod-like structural characteristics, PPES formed a helical superstructure around the SWNT surface, manifested by both the molecular dynamics (MD) simulation and the experimental microscopic measurements. Observed pitches of helices of wrapped PPES were found to be 5-15 and ~25 nm by TEM and AFM, respectively, while MD simulation with (10,0)-SWNT predicted 14 ± 1 nm. These results revealed that the hydrophilic side chains of PPES along with the van der Waals interaction between the backbone of PPES and SWNT play an important role in the dispersion of SWNT's, a key step in carbon nanotube processing and engineering.

11. Block Copolymer Nanotemplates for Biomolecular arrays

Jung Hyun Park, Yujie Sun, Yale E. Goldman, Russell J. Composto,

The biological motor system consisting of myosin and actin filaments is inherently a nanoscale machine. By harnessing this biologically inspired nanotechnology, the next-generation of lab-on-a-chip designs can be powered by active transport of payloads. Because of their spatial dimensions and orientation, the perpendicular lamellar structure of diblock copolymer films deposited on silicon substrates is a good candidate as a nanotemplate that can guide the alignment of single actin filaments and myosin. Using scanning probe microscopy, a nearly symmetric poly(styrene-b-methyl methacrylate) P(S-b-MMA) diblock copolymer spin coated on silicon and annealed at 175°C for 2 days exhibits a perpendicular lamellar morphology with a periodicity of 70nm. To further constrain actin and/or myosin, topographical variations were etched into the film by exposure to UV radiation for varying times. This exposure was found to preferentially etch the MMA phase resulting in "trenches" of MMA stripes separated by hills of PS. Studies are underway to investigate the alignment of actin on both the perpendicular lamellar morphology and the same morphology with trenches.

12. Design of functional ferritin-like proteins

Joe Swift, Christopher A. Butts, Seung-gu Kang, Lei Zhang, Jeffery G. Saven, Ivan J. Dmochowski

One of the challenges facing the nanotechnology community is the ability to structure and position nanomaterials within larger size domains. The self-assembly properties of proteins and biological systems offer a potential solution to this problem. Ferritin four-helix bundle subunits assemble to create a stable multimer with a large cavity where metal ions bind. We have shown that wild-type ferritins form gold and silver nano-

particles exterior to the protein shell. Computer analysis guided the positioning of several new cysteines on the interior surface of human H ferritin. These new proteins have been shown to be correctly assembled, stable and have been extensively characterized. We also present data supporting the formation of noble metal nanoparticles within the cavity. Ferritin offers an ideal model system with which to study the processes of seeding and growth in the growing field of protein-directed nanoparticle templating.

13. Title: Tracking Myosin Motors on Actin Filaments in 3D

Yujie Sun, Yale E. Goldman

Myosin V and VI are motor proteins that move processively on actin filaments. There has been evidence showing that myosin molecules often walk in an irregular manner due to the stochastic nature of their stepping and complex actin networks. Tracking single myosin molecular motors in 3D is indispensable to address their stepping mechanisms in vivo.

We have developed a technique, PARALLAX VIEW, to track single fluorescent labeled molecules in 3D with good spatial resolution. A preliminary application of this technique on myosin V and VI shows interesting difference in stepping patterns between the two myosin motors.

14. Structure and activity of apoferritin-stabilized gold nanoparticles

Lei Zhang, Ivan Dmochowski

Horse spleen apoferritin (HSAF) has been used to template the synthesis of various inorganic nanoparticles inside its 8-nm cavity. However, the present study is the first detailed report on the addition and reduction of Au^{3+} to form Au^{0} nanoparticles outside of HSAF. A simple method for synthesizing gold nanoparticles stabilized by HSAF is reported using $NaBH_4$ or 3-(N-morpholino)propanesulfonic acid (MOPS) as the reducing agent. $AuCl_4^-$ reduction by $NaBH_4$ was complete within a few seconds, whereas reduction by MOPS was much slower; in all cases, protein was required during reduction to keep the gold particles in aqueous solution. High-resolution transmission electron microscopy (TEM) showed that the gold nanoparticles were associated with the outer surface of the protein. The average particle diameters were 3.6 and 15.4 nm for $NaBH_4$-reduced and MOPS-reduced Au-HSAF, respectively. A 5-nm difference in the UV-Vis absorption maximum was observed for $NaBH_4$-reduced (530 nm) and MOPS-reduced Au-HSAF (535 nm), which was attributed to the greater size and aggregation of the MOPS-reduced gold sample. $NaBH_4$-reduced Au-HSAF was much more effective than MOPS-reduced Au-HSAF in catalyzing the reduction of 4-nitrophenol by $NaBH_4$, based on the greater accessibility of the $NaBH_4$-reduced gold particle to the substrate. Rapid reduction of $AuCl_4^-$ by $NaBH_4$ was determined to result in less surface passivation by the protein.